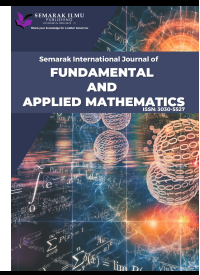




Semarak International Journal of Fundamental and Applied Mathematics

Journal homepage:
<https://semarakilmu.my/index.php/sijfam>
ISSN: 3030-5527



Dual Solution Analysis of Magnetohydrodynamic Flow and Heat Transfer over a Stretching/Shrinking Cylinder in CNT Nanofluids

Aina Anisah Ahmad Sidin¹, Norfifah Bachok^{2,*}, Nur Syahirah Wahid², Mohd Shafie Mustafa², Ioan Pop³

¹ Institute for Mathematical Research, Universiti Putra Malaysia, 43400 Serdang, Selangor, Malaysia

² Department of Mathematics and Statistics, Faculty of Science, Universiti Putra Malaysia, 43400 Serdang, Selangor, Malaysia

³ Department of Mathematics, Babes-Bolyai University, 400084 Cluj-Napoca, Romania

ARTICLE INFO

Article history:

Received 8 June 2025

Received in revised form 29 July 2025

Accepted 10 August 2025

Available online 25 August 2025

Keywords:

Carbon nanotubes;
magnetohydrodynamic; heat transfer;
stretching or shrinking cylinder; dual
solutions

ABSTRACT

The study of flow over a stretching/shrinking cylinder at stagnation point considering the effect of magnetohydrodynamic investigated. The governing equations, along with the boundary conditions, were transformed into ordinary differential equations using a similarity transformation. These equations were then solved using the *bvp4c* in MATLAB. Two base fluids, water and kerosene and both single-wall (SWCNTs) and multi-wall (MWCNTs) carbon nanotubes, each with distinct densities. The effects of several parameters were examined through graphical representations of velocity, temperature, skin friction coefficients and heat transfer rate. These parameters include the magnetic field M , curvature parameter γ , stretching/shrinking parameter λ and CNT volume fraction ϕ . The findings illustrated that dual solutions exist for shrinking case and unique solution present in stretching case. The heat transfer rates are higher in kerosene-based fluid with single-walled carbon nanotubes compared to water-based fluid with multi-walled carbon nanotubes.

1. Introduction

The field of research involving cylindrical surfaces has been extensively explored in previous studies. For instance, Norkin [1] investigated how cavities form when a circular cylinder first moves through a fluid with constant acceleration. Kostikov and Makarenko [2] considered the unsteady free surface flow above a moving circular cylinder. The role of rotating cylinders has also attracted considerable attention, as highlighted by Selimefendigil and Chamkha [3], who examined a 3D magnetohydrodynamic vented cavity featuring surface corrugation and an inner rotating cylinder. Additional studies on rotating cylindrical surfaces include in other studies [4-7].

Research on stretching or shrinking cylinders is relatively new and still being explored. However, these cylinders are widely used in various engineering fields, such as biomedical engineering and chemical processing. They are utilized in biomechanics and tissue engineering studies, including

* Corresponding author.

E-mail address: norfifah@upm.edu.my

research on blood vessels and muscles. Additionally, stretching or shrinking cylinder are employed in chemical reactors for vessel deformation and flow channel analysis. The study of stretching or shrinking cylinder can be founded by few authors, such as Wang [8] studied the the fluid flow outside of a stretching cylinder. Ashorynejad *et al.*, [9] found that adding copper, silver, alumina, or titanium oxide nanoparticles to water flowing around an expanding cylinder under a magnetic field improved cooling. Mukhopadhyay [10] analyzes the flow and thermal characteristics of boundary layer axisymmetric flow along a stretching cylinder under the combined influence of slip and a uniform magnetic field. The findings of the study, it is found that the velocity decreases with increasing velocity slip parameter and magnetic parameter. The skin friction as well as the heat transfer rate at the surface is larger for a cylinder compared to a flat plate. Then, Najib *et al.*, [11] investigated the stagnation point flow and mass transfer with chemical reaction past a stretching/shrinking cylinder. Next, axisymmetric flow of a viscous incompressible fluid over a shrinking vertical cylinder with heat transfer is investigated by Mishra and Singh [12]. Mat *et al.*, [13] examined the boundary layer stagnation-point slip flow and heat transfer along a shrinking/stretching cylinder over a permeable surface found that velocity and temperature profiles increase as the curvature parameter increases. Khashi'ie *et al.*, [14] hybrid nanofluid flow past a shrinking cylinder with prescribed surface heat flux and stated that flat plate surface abates the separation of boundary layer while it enhances the heat transfer process. Awaludin *et al.*, [15] also shows an interest in study the steady stagnation point flow and heat transfer passes a horizontal shrinking permeable cylinder. It stated that given the existence of dual solutions in the present study for a certain range of the curvature parameter. Kardri *et al.*, [16] investigated the magnetohydrodynamic (MHD) stagnation point flow and heat transfer around a nonlinear stretching or shrinking cylinder in nanofluids, incorporating the effects of viscous dissipation and internal heat generation by applying the Tiwari-Das model.

Choi and Eastman [17] initially use the term "nanofluid," referring to a fluid containing nanoscale particles with dimensions less than 100 nanometers. Nanofluids have a significant impact on research applications owing to their enhanced thermal conductivity, which improves heat transfer rates and efficiency in heat exchange systems. Arifin *et al.*, [18] expressed interest in investigating viscous flow induced by a permeable stretching/shrinking sheet in a nanofluid, an extension initially proposed by Wang [19] from the original work of Tiwari and Das [20]. Copper and silver are examined as nanoparticles to explore the impact of nanoparticle volume fraction on the flow and the characteristics of heat transfer. The explore of research in using nanofluid can be seen in the papers by Bachok *et al.*, [21], Makinde and Aziz [22], Bachok *et al.*, [23] and Bachok *et al.*, [24]. Carbon nanotubes (CNTs) have exceptionally high thermal conductivity as stated by Iijima [25], several times greater than copper or silver nanoparticles. This property makes them highly effective in enhancing heat transfer rates in nanofluids, leading to improved thermal management in various systems. It was stated by Halelfadl *et al.*, [26] that nanofluids could offer advantages in energy systems and heat exchangers where fluid flow aligns with the setup's temperature, the volume fraction of nanoparticles and flow regimes. In a study by Norzawary *et al.*, [27], the effects of suction and injection on flow over stretching/shrinking surfaces were examined using single-walled carbon nanotubes (SWCNTs), multi-walled carbon nanotubes (MWCNTs), and water-based fluids. The results indicated that increasing suction and nanoparticle volume fraction enhances the heat transfer rate at the surface. Additionally, SWCNTs demonstrated superior performance in terms of skin friction coefficient and heat transfer compared to MWCNTs. Meanwhile, Mahabaleshwar *et al.*, [28] discovered that SWCNTs outperform MWCNTs in SWCNT-MWCNT/water flow over stretching/shrinking surfaces influenced by hydromagnetic effects. Samat *et al.*, [29] concluded in their study on CNT flow over a stretching/shrinking porous surface under the influence of MHD effects that an increase in the magnetic field leads to higher skin friction and enhanced heat transfer.

Many researchers have shown an interest in studying carbon nanotubes in various flow scenarios, including rotational flow [30-33] and exponential stretching/shrinking [34].

Few studies have considered the effects of magnetohydrodynamics. Mahapatra and Gupta [35] explored the steady two-dimensional stagnation-point flow of an incompressible viscous electrically conducting fluid toward a stretching surface, with the flow permeated by a uniform transverse magnetic field. Subsequently, Aman *et al.*, [36] examined stagnation point flow past a stretching/shrinking sheet with the availability of magnetohydrodynamic effect and slip effect. They obtained results indicating that the presence of slip effects causes the skin friction coefficients to decrease and the heat transfer rate to increase. The main objective was to observe the non-unique solution, which was found to exist for a shrinking sheet, while a unique solution was observed for a stretching sheet. Moreover, Anuar *et al.*, [37] investigated the influence of MHD and a nonlinear parameter on nonlinear stretching or shrinking in single-walled carbon nanotubes (SWCNTs) and multi-walled carbon nanotubes (MWCNTs), incorporating kerosene and water as base fluids. The findings of this study illustrated that SWCNTs perform better than MWCNTs in terms of skin friction and surface heat transfer rate. A similar trend was observed with increasing magnetic field strength, which led to increased skin friction and heat transfer. Other researchers have shown interest in considering magnetic field effects on stagnation point flow in their research, as evidenced by the works of Ishak *et al.*, [38] and Uddin *et al.*, [39]. In addition, the effects of hydromagnetic are also implemented on stretching/shrinking surfaces as evaluated in Yasin *et al.*, [40]. These authors found that the availability of magnetic field in the study of MHD and radiation past a permeable stretching/shrinking sheet cause the skin friction coefficient to increase. Furthermore, Patel *et al.*, [41] studied a micropolar ferrofluid in the presence of a magnetic field over a stretching/shrinking sheet. Yashkun *et al.*, [42] conducted research on a stretching/shrinking surface in a hybrid nanofluid, focusing on the effects of suction and radiation. For further studies on MHD over a stretching/shrinking sheet, also refer to the works of Zhang *et al.*, [43] and Vishalakshi *et al.*, [44].

This study focuses on analyzing stagnation point flow over a stretching or shrinking cylinder in carbon nanotube-based fluids, incorporating the effects of a magnetic field. This is a combination of ideas from Kardri *et al.*, [16], Samat *et al.*, [29] and Anuar *et al.*, [37] explores a research that has not yet been investigated. The governing equations are converted into ordinary differential equations using a similarity transformation and are solved numerically. The influence of various key parameters on the heat transfer rate is analyzed and illustrated through graphical results.

2. Formulation of the Problem

Consider the two-dimensional magnetohydrodynamic flow past a linearly stretching/shrinking cylinder at a stagnation point. This study incorporates both single-walled carbon nanotubes (SWCNTs) and multi-walled carbon nanotubes (MWCNTs) as nanoparticles, with water and kerosene as the base fluids. The free stream velocity is defined as $U_\infty = bx$, where b is a constant and the cylinder of radius R is immersed in an incompressible nanofluid of constant temperature, T_w . The stretching/shrinking velocity is expressed as $U_w = ax$, where a is a constant.

The thermophysical properties of SWCNT and MWCNT are compared between water and kerosene. These fluids were selected for comparison with previous studies.

Table 1

Thermophysical properties of based fluids and CNTs [45]

Physical Properties	Base Fluids		Nanoparticle	
	Water ($Pr = 6.2$)	Kerosene ($Pr = 21$)	SWCNT	MWCNT
$\rho(kg/m^3)$	997	783	2600	1600
$c_p(J/kgK)$	4179	2090	425	796
$k(W/mK)$	0.613	0.145	6600	3000

The governing equations consist of continuity, momentum and energy equations are expressed based on the formulation by Kardri *et al.*, [16] as follows:

$$\frac{\partial(ru)}{\partial x} + \frac{\partial(rv)}{\partial r} = 0, \quad (1)$$

$$u \frac{\partial u}{\partial x} + v \frac{\partial v}{\partial r} = U_\infty \frac{dU_\infty}{dx} + \left(\frac{\mu_{nf}}{\rho_{nf}} \right) \left(\frac{\partial^2 u}{\partial r^2} + \left(\frac{1}{r} \right) \frac{\partial u}{\partial r} \right) + \frac{\sigma B_o^2}{\rho_{nf}} (U_\infty - u), \quad (2)$$

$$u \frac{\partial T}{\partial x} + v \frac{\partial T}{\partial r} = \alpha_{nf} \left(\frac{\partial^2 T}{\partial r^2} + \left(\frac{1}{r} \right) \frac{\partial T}{\partial r} \right), \quad (3)$$

subject to the boundary conditions of the following problem

$$\begin{aligned} u &= U_w, \quad v = 0, \quad T = T_w \quad \text{at } r = R, \\ u &\rightarrow U_\infty, \quad T \rightarrow T_\infty \quad \text{as } r \rightarrow \infty, \end{aligned} \quad (4)$$

where u and v are the velocity components in the x and r directions, respectively and T denoted for fluid temperature. the subscripts nf , f and CNT denote nanofluids, fluids and carbon nanotubes, respectively. Additionally, α represents the thermal diffusivity, μ stands for dynamic viscosity, ρ for the density, C_p signifies specific heat at constant pressure, k denotes thermal conductivity and φ indicates nanoparticle volume fraction, as illustrated below Oztop *et al.*, [46]:

$$\begin{aligned} \mu_{nf} &= \frac{\mu_f}{(1-\varphi)^{2.5}}, \quad \rho_{nf} = (1-\varphi)\rho_f + \varphi\rho_{CNT}, \\ \alpha_{nf} &= \frac{k_{nf}}{(\rho C_p)_{nf}}, \quad (\rho C_p)_{nf} = (1-\varphi)(\rho C_p)_f + \varphi(\rho C_p)_{CNT}, \\ k_{nf} &= \frac{1-\varphi + 2\varphi \frac{k_{CNT}}{k_{CNT}-k_f} \ln \frac{k_{CNT}+k_f}{2k_f}}{1-\varphi + 2\varphi \frac{k_f}{k_{CNT}-k_f} \ln \frac{k_{CNT}+k_f}{2k_f}} \times k_f. \end{aligned} \quad (5)$$

Additionally, the Eq. (6) presented the similarity variables that are use to solve the governing equations, Eq. (1) – (3) along with the boundary conditions, Eq. (4).

$$\eta = \frac{r^2 - R^2}{2R} \left(\frac{b}{v_f} \right)^{\frac{1}{2}}, \quad \psi = (bv_f)^{\frac{1}{2}} x R f(\eta), \quad \theta(\eta) = \frac{T - T_\infty}{T_w - T_\infty}, \quad v_f = \frac{\mu_f}{\rho_f}. \quad (6)$$

The governing equations of the momentum and energy equations from Eqs. (2) and (3) are reduced to a set of ordinary differential equations (ODEs) through the implementation of Eq. (5) along with similarity transformations, Eq. (6), resulting ODEs and their corresponding boundary conditions are provided in Eq. (7):

$$\frac{1}{(1-\varphi)^{2.5}[(1-\varphi) + \varphi\rho_{CNT}/\rho_f]} [(1+2\gamma\eta)f''' + 2\gamma f''] + ff'' - f'^2 + M(1-f') + 1 = 0, \quad (7)$$

$$\frac{1}{Pr} \frac{k_{nf}/k_f}{[(1-\varphi) + \varphi(\rho C_p)_{CNT}/(\rho C_p)_f]} [(1+2\gamma\eta)\theta'' + 2\gamma\theta'] + f\theta' = 0, \quad (8)$$

$$\begin{aligned} f(0) &= 0, \quad f'(0) = \varepsilon, \quad \theta(0) = 1, \\ f'(\eta) &\rightarrow 1, \quad \theta(\eta) \rightarrow 0, \quad \text{as } \eta \rightarrow \infty, \end{aligned} \quad (9)$$

where the external magnetic field is $M = \sigma B_o^2 / \rho_{nf} b$, where B_o is a constant, Pr represents the Prandtl number and γ denotes the curvature parameter. The parameter for the shrinking or stretching surface is designated as λ , where $\lambda > 0$ corresponds to the stretching case while $\lambda < 0$ corresponds to the shrinking case.

$$Pr = \frac{\nu_f}{\alpha_f}, \quad \gamma = \left(\frac{\nu_f x^{(1-n)}}{bR^2} \right)^{\frac{1}{2}}. \quad (10)$$

The local skin friction coefficients, C_f and local Nusselt number, Nu_x are demonstrated as follow:

$$C_{fx} = \frac{\tau_w}{\rho_f U_\infty^2}, \quad (11)$$

$$Nu_x = \frac{xq_w}{k_f(T_w - T_\infty)}. \quad (12)$$

Given the shear stress of the surface τ_w and heat flux q_w as:

$$\tau_w = \mu_{nf} \left(\frac{\partial u}{\partial r} \right)_{r=R}, \quad q_w = -k_{nf} \left(\frac{\partial T}{\partial r} \right)_{r=R}. \quad (13)$$

The physical quantities below obtained by applying Eqs. (11) – (13).

$$Re_x^{\frac{1}{2}} C_f = \frac{1}{(1-\varphi)^{2.5}} f''(0), \quad (14)$$

$$Re_x^{-\frac{1}{2}} Nu_x = -\frac{k_{nf}}{k_f} \theta'(0), \quad (15)$$

where $Re_x = U_\infty x / \nu_f$ refers to the local Reynolds number.

3. Analysis of Results

The nonlinear ordinary differential equations (ODEs) Eqs. (7) and (8), along with boundary conditions Eq. (9), were obtained using the boundary value problem solver (bvp4c) in MATLAB. Based on Table 2, the values of the $f''(0)$ can be compared between the study by Anuar *et al.*, [37] and current study, considering $\gamma = \varphi = M = 0$ for water-SWCNT. The consistent results obtained for $\gamma = 0$ in both studies indicate validation, with both results being compatible. Dual solutions can be found within the range of parameter influences such as $0.1 \leq \varphi \leq 0.2$, $0 \leq \gamma \leq 0.02$ and $0 \leq M \leq 0.05$ as stated in Kardri *et al.*, [16] and Anuar *et al.*, [37]. This study also considers stretching or shrinking cases with the parameter λ . As can be seen in Table 1, it provides a comprehensive overview of the thermophysical characteristics of both types of carbon nanotube with two base fluids: water and kerosene. This includes their respective values for density, specific heat at constant temperature and thermal conductivity. In addition, this study contributes to the determination of the Prandtl number, which exhibits variability based on the chosen base fluids. Specifically, Pr is defined as $Pr = 6.2$ for water and $Pr = 21$ for kerosene. Thus, further explanations and results can be explored by illustrating the graphical results of the velocity profile, temperature profile, skin friction coefficients and local Nusselt in Figures 1 – 14.

Table 2

Comparison values of $f''(0)$ for different λ and γ when $\varphi = M = 0$ for water-SWCNT

λ	Anuar <i>et al.</i> , [37]		Present Results	
	$\gamma = 0$	$\gamma = 0$	$\gamma = 0.01$	$\gamma = 0.02$
2	-1.887307	-1.887307	-1.891910	-1.896505
1	0	0	0	0
0.5	0.713295	0.713295	0.715845	0.718387
0	1.232588	1.232588	1.238042	1.243475
-0.5	1.495670	1.495670	1.504878	1.514029
-1.0	1.328817	1.328817	1.345669	1.362272
-1.15	1.082231	1.082231	1.107213	1.131379
	[0.116702]	[0.116702]	[0.105222]	[0.094413]
-1.2	0.932473	0.932473	0.965974	0.997447
	[0.233650]	[0.233650]	[0.213369]	[0.195019]
-1.2465	0.584282	0.584281	0.721074	0.786771
	[0.554296]	[0.554296]	[0.430615]	[0.377963]

[] : Second solution

3.1 Reduced Skin Friction Coefficients and Heat Transfer

Figures 1 and 2 show the graphical results of the reduced skin friction coefficients $f''(0)$ and reduced heat transfer $-\theta'(0)$ for variation value of M and stretching/shrinking parameter λ , considering water-SWCNT. The magnetic parameter $M = 0, 0.02$ and 0.5 , with corresponding critical values of λ_c achieved at $-1.30628, -1.27978$ and -1.26215 , respectively. The value of $M = 0$ indicates flow without magnetic field effects in the fluid flow. The dual solutions are more widen in $M = 0$ compared to $M = 0.02$ and 0.05 . These dual solutions exist within the range of $\lambda_c < \lambda \leq -1.0$, while no solution can be obtained when $\lambda < \lambda_c$. The reduced skin friction coefficients and reduced heat transfer increase as the value of M increase and decelerating the thermal boundary layer separation process.

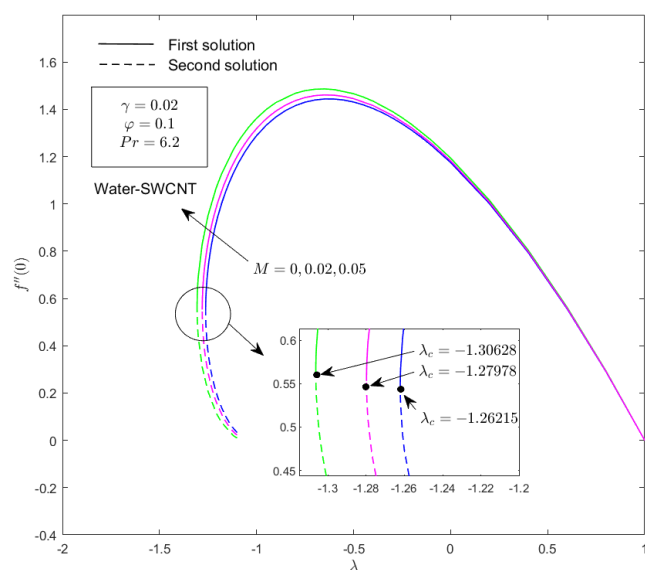


Fig. 1. Reduced skin friction coefficients $f''(0)$ for various values of M

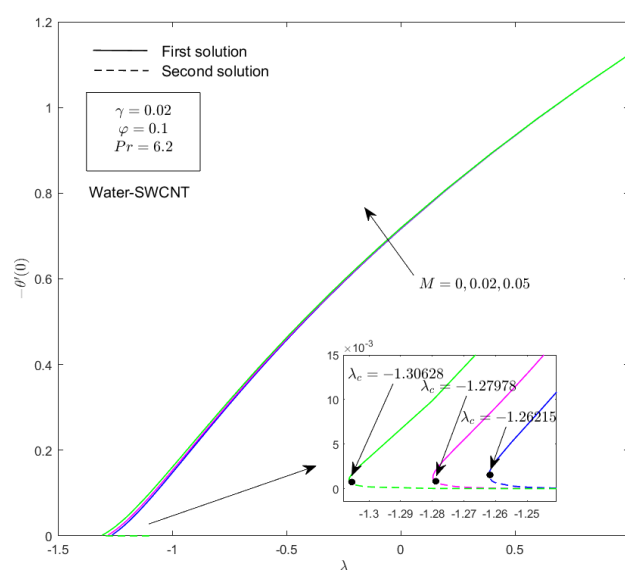


Fig. 2. Reduced heat transfer $-\theta'(0)$ for various values of M

Figures 3 and 4 exhibit the reduced skin friction coefficients and reduced heat transfer for different values of the curvature parameter γ along the stretching/shrinking parameter λ for water-MWCNT, for several values of γ when $M = 0.02$ and $\varphi = 0.1$. The reduced skin friction coefficients increase while the reduced heat transfer decreases as γ increases in value. Additionally, the critical values λ_c also decrease. The dual solutions exist for $\lambda_c < \lambda \leq -1.0$ and unique solution only exist when $\lambda > -1.0$. Since, $\lambda > 0$ represents a stretching case, while $\lambda < 0$ represents a shrinking case, it can be concluded that dual solutions exist in the shrinking case, while uniqueness exists in the stretching case.

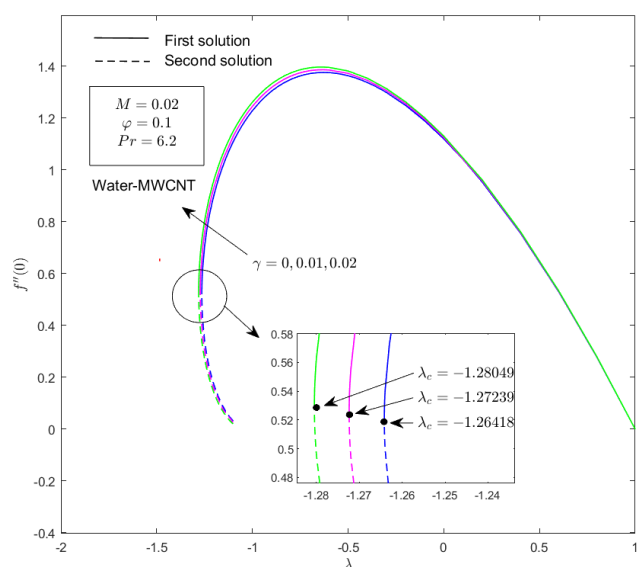


Fig. 3. Reduced skin friction coefficients $f''(0)$ for various values of γ

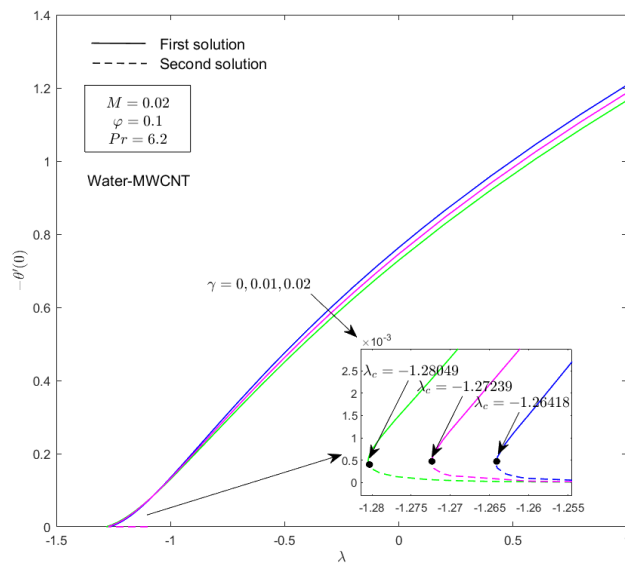


Fig. 4. Reduced heat transfer $-\theta'(0)$ for various values of γ

3.2 Local Skin Friction Coefficients and Local Nusselt Number

The variations of local skin friction coefficients $Re_x^{\frac{1}{2}}C_f$ and local Nusselt number $Re_x^{-\frac{1}{2}}Nu_x$ with nanoparticle volume fraction are provided in Figures 5 – 10 with the different values of M , γ and different types of based fluid and carbon nanotubes. The figures consider two distinct base fluids, water and kerosene and two varieties of carbon nanotubes (single-walled CNTs and multi-walled CNTs), within a shrinking case ($\lambda = -1.2$). The graphical results in Figures 5 and 6 illustrate the outcomes of the local skin friction coefficients and local Nusselt number for different values of M when $\gamma = 0.02$ for single-walled CNTs. The local skin friction coefficients and local Nusselt number increase in both water- and kerosene-based fluid as M increases. In Figure 5, it is observed that kerosene produced higher local skin friction coefficients compared to water-based fluid. However, an opposite trend is shown for both base fluids in Figure 6 as water produced a higher heat transfer rate.

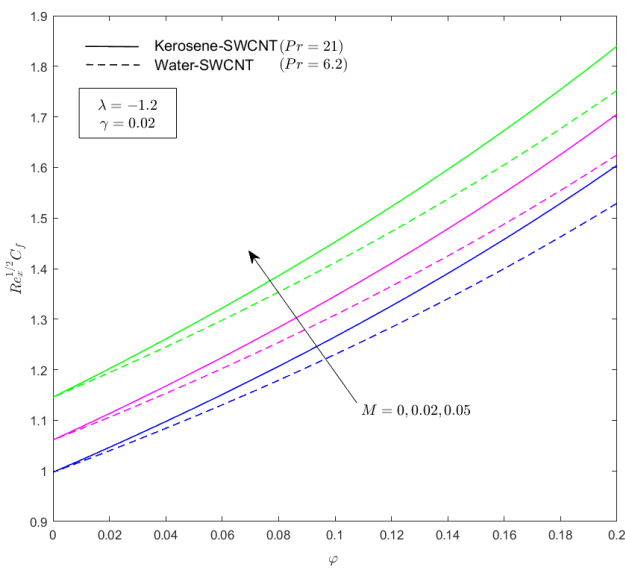


Fig. 5. Variation of $Re_x^{\frac{1}{2}}C_f$ with ϕ for various values of M

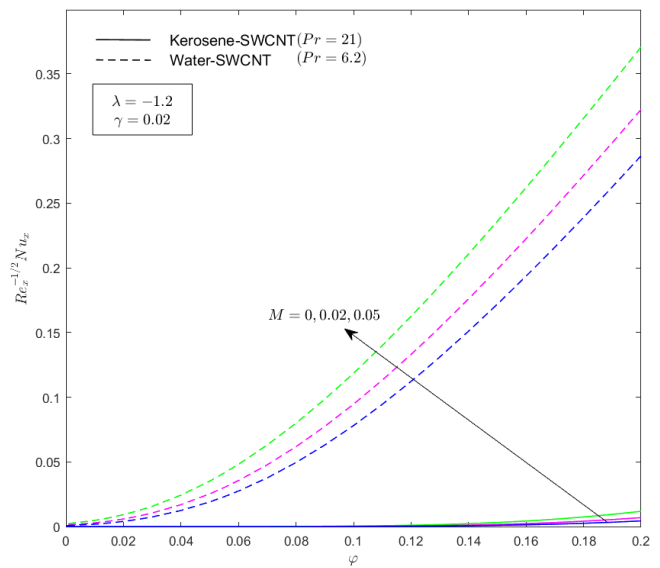


Fig. 6. Variation of $Re_x^{-\frac{1}{2}}Nu_x$ with ϕ for various values of M

Next, based on Figures 7 and 8, it shows the effects of varying curvature parameter γ values on local skin friction coefficients and local Nusselt number when $M = 0.02$. The value $\gamma = 0.01$ and 0.02 are taken to represent existence of the curvature parameter, while $\gamma = 0$ represents a flat surface. Figure 7 it is revealed that kerosene-based fluid exhibits a higher local skin friction coefficients than water-based fluid. Conversely, water-base fluid single-wall CNTs demonstrate a greater heat transfer rate compared to kerosene-based fluid single-wall CNTs as illustrated in Figure 8.

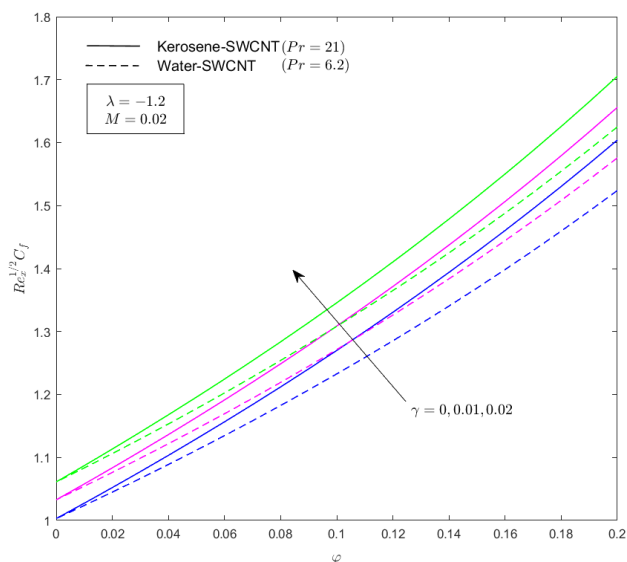


Fig. 7. Variation of $Re_x^{\frac{1}{2}} C_f$ with ϕ for various values of γ

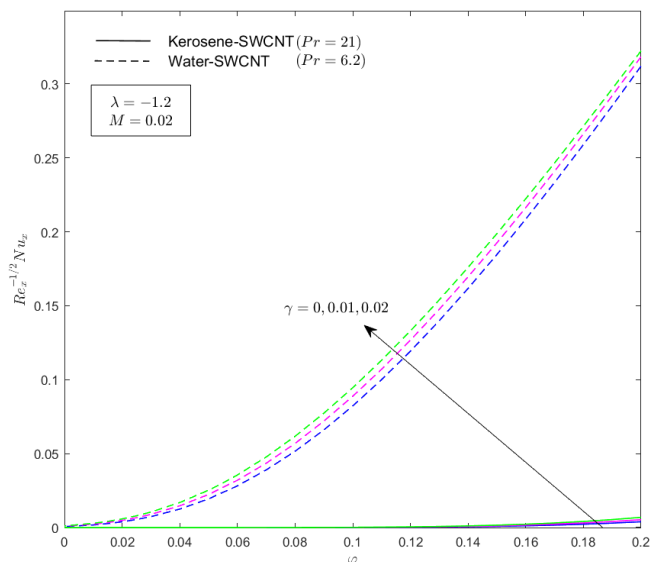


Fig. 8. Variation of $Re_x^{-\frac{1}{2}} Nu_x$ with ϕ for various values of γ

Figures 9 and 10 further compare the performance of different base fluids and CNT types. This comparison indicates that water-based fluid yielded much lower local skin friction coefficients and higher heat transfer, whereas single-walled CNTs exhibited higher local skin friction coefficients and heat transfer.

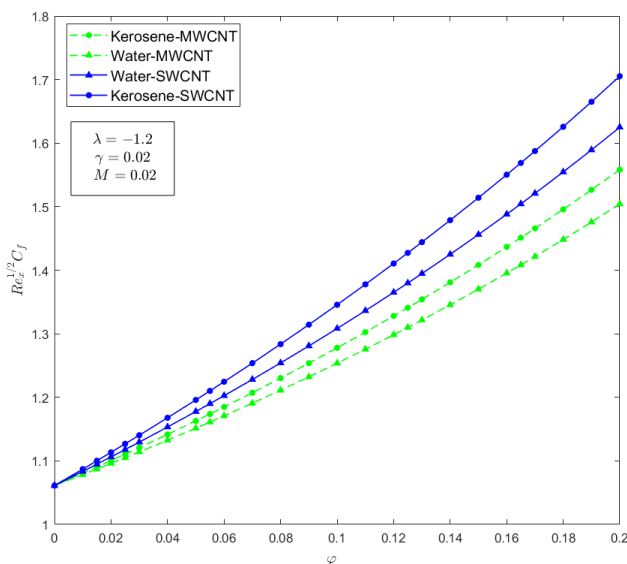


Fig. 9. Variation of $Re_x^{\frac{1}{2}} C_f$ with ϕ for various nanoparticles

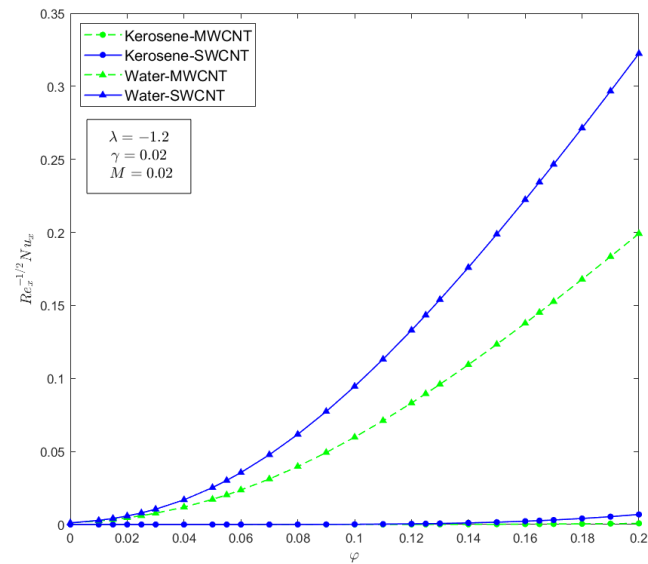


Fig. 10. Variation of $Re_x^{-\frac{1}{2}} Nu_x$ with ϕ for various nanoparticles

3.3 Local Skin Friction Coefficients and Local Nusselt Number

The velocity $f'(\eta)$ and temperature profiles $\theta(\eta)$ for various values of nanoparticle volume fraction φ and magnetic field parameter M illustrated in Figures 11 and 12. The values of $M = 0$ and 0.02 are compared with different values of $\varphi = 0.1, 0.15, 0.2$. From the obtained graphs, it is revealed that with an increase in the value of φ , the velocity profiles decrease, while there is an opposite trend for temperature profiles, which increase. It is observed from the figures that the presence M decreases and increases both profiles, respectively, compared to $M = 0$.

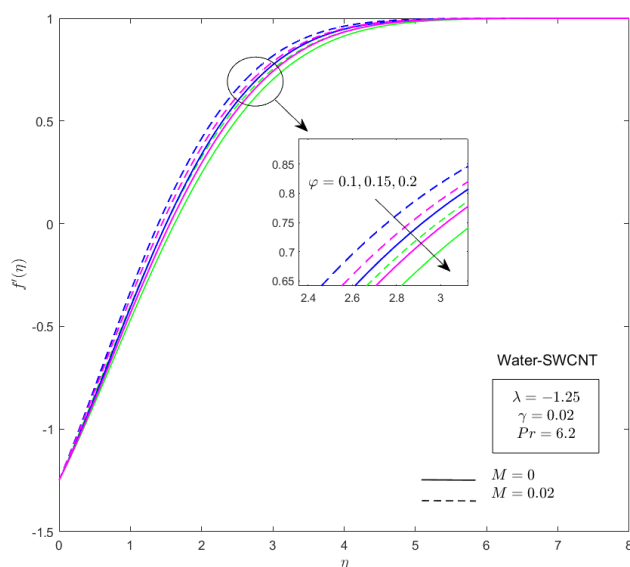


Fig. 11. Velocity profiles for various values of φ and M

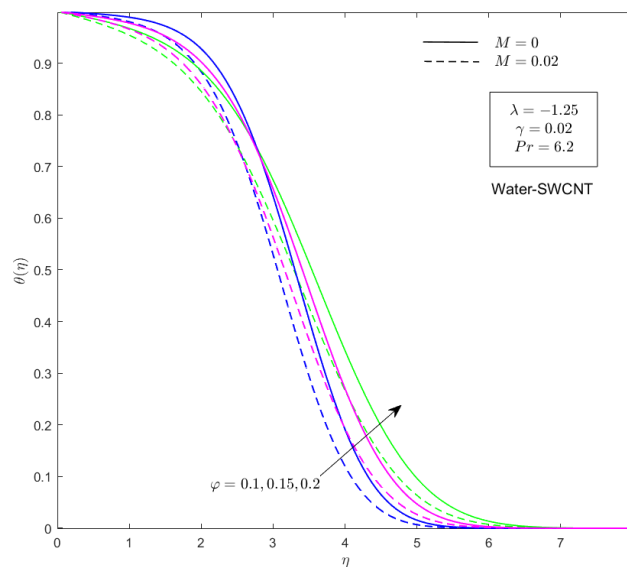


Fig. 12. Temperature profiles for various values of φ and M

Figures 13 and 14 display the impact of nanoparticle volume fraction φ and curvature parameter γ on velocity and temperature profiles. The curvature parameter is varied, with $\gamma = 0$ representing a flat surface and $\gamma = 0.01$ representing the presence of curvature. The influence of curvature parameter γ affects the velocity to be higher and the temperature profiles to be lower than those on the flat surface ($\gamma = 0$). It is observed from the figures that an increase in volume fraction of nanoparticles leads to a decrease in velocity profiles and an increase in the temperature profiles of the flow. This occurs because the increase in nanoparticle volume is associated with a decrease in the thickness of the velocity boundary layer adjacent to the walls, due to higher friction. Additionally, it enhances the thermal conductivity of the flow, resulting in an increase in temperatures.

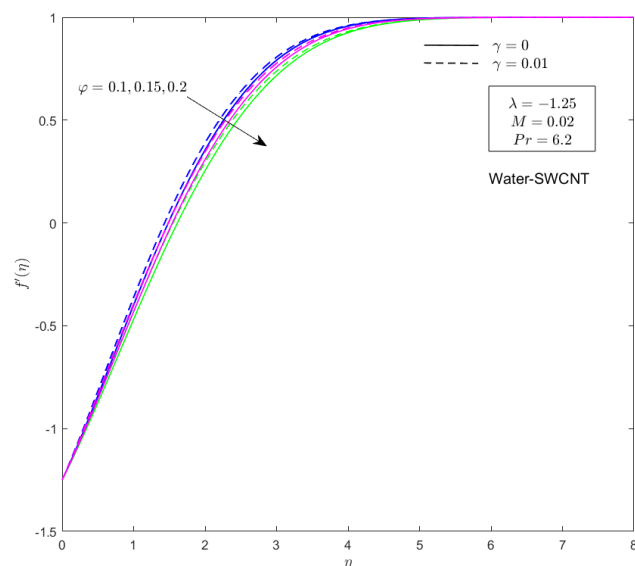


Fig. 13. Velocity profiles for various values of φ and γ

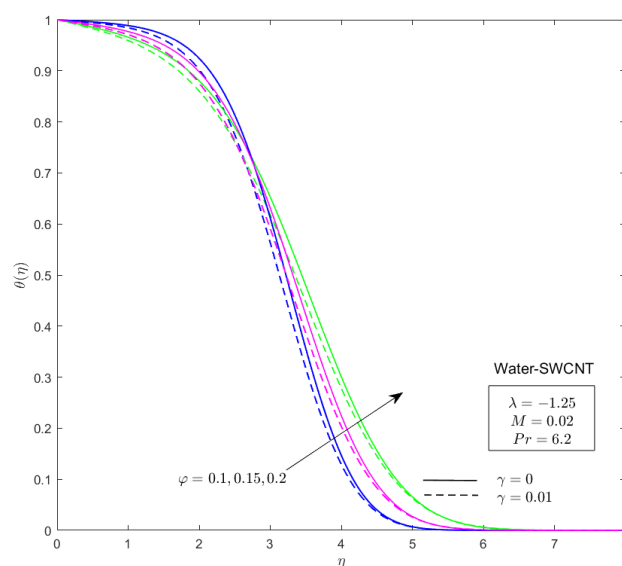


Fig. 14. Temperature profiles for various values of φ and γ

4. Conclusions

The behavior of SWCNT-MWCNT nanoparticles across linearly stretching/shrinking cylinder with the effects of hydromagnetic is studied in this research. The graphical results are obtained with reference to several parameters and include plots of reduced skin friction coefficients, reduced heat transfer, local skin friction coefficients, local Nusselt number, as well as velocity and temperature profiles. The findings can be summarized as follows:

- i. Non-unique solutions exist for shrinking case $\lambda < 0$, while unique solutions are obtained for stretching case $\lambda > 0$.
- ii. Increasing the values of M and γ results in higher skin friction coefficients and heat transfer rates.
- iii. Kerosene-based fluid contribute to higher skin friction coefficients and heat transfer compared to water-based fluid.
- iv. SWCNTs provide better skin friction coefficients and heat transfer compared to MWCNTs.

Acknowledgement

The authors gratefully acknowledge the financial support received from Universiti Putra Malaysia (GP-GPB9784400).

References

- [1] Norkin, M. B. "Formation of a cavity in the initial stage of motion of a circular cylinder in a fluid with a constant acceleration." *Journal of Applied Mechanics and Technical Physics* 53, no. 4 (2012): 532-539. <https://doi.org/10.1134/S0021894412040074>.
- [2] Kostikov, V. K., and N. I. Makarenko. "Unsteady free surface flow above a moving circular cylinder." *Journal of Engineering Mathematics* 112, no. 1 (2018): 1-16. <https://doi.org/10.1007/s10665-018-9962-x>.
- [3] Selimefendigil, Fatih, and Ali J. Chamkha. "MHD mixed convection of nanofluid in a three-dimensional vented cavity with surface corrugation and inner rotating cylinder." *International Journal of Numerical Methods for Heat & Fluid Flow* 30, no. 4 (2020): 1637-1660. <https://doi.org/10.1108/HFF-10-2018-0566>.
- [4] Hansen, Erik B., and Mark A. Kelmanson. "Steady, viscous, free-surface flow on a rotating cylinder." *Journal of Fluid mechanics* 272 (1994): 91-108. <https://doi.org/10.1017/S0022112094004398>.

- [5] Hosoi, A. E., and L. Mahadevan. "Axial instability of a free-surface front in a partially filled horizontal rotating cylinder." *Physics of Fluids* 11, no. 1 (1999): 97-106. <https://doi.org/10.1063/1.869905>.
- [6] Mittal, Sanjay, and Bhaskar Kumar. "Flow past a rotating cylinder." *Journal of fluid mechanics* 476 (2003): 303-334. <https://doi.org/10.1017/S0022112002002938>.
- [7] Silverman, D. C. "The rotating cylinder electrode for examining velocity-sensitive corrosion—a review." *Corrosion* 60, no. 11 (2004): 1003-1023. <https://doi.org/10.5006/1.3299215>.
- [8] Wang, Ch Y. "Fluid flow due to a stretching cylinder." *Physics of Fluids* 31, no. 3 (1988): 466-468.. <https://doi.org/10.1063/1.866827>.
- [9] Ashorynejad, H. R., M. Sheikholeslami, I. Pop, and D. D. Ganji. "Nanofluid flow and heat transfer due to a stretching cylinder in the presence of magnetic field." *Heat and Mass Transfer* 49, no. 3 (2013): 427-436. <https://doi.org/10.1007/s00231-012-1087-6>.
- [10] Mukhopadhyay, Swati. "MHD boundary layer slip flow along a stretching cylinder." *Ain Shams Engineering Journal* 4, no. 2 (2013): 317-324. <https://doi.org/10.1016/j.asej.2012.07.003>.
- [11] Najib, Najwa, Norfifah Bachok, Norihan Md Arifin, and Anuar Ishak. "Stagnation point flow and mass transfer with chemical reaction past a stretching/shrinking cylinder." *Scientific reports* 4, no. 1 (2014): 4178. <https://doi.org/10.1038/srep04178>.
- [12] Mishra, Upendra, and Gurinder Singh. "Dual solutions of mixed convection flow with momentum and thermal slip flow over a permeable shrinking cylinder." *Computers & Fluids* 93 (2014): 107-115. <https://doi.org/10.1016/j.compfluid.2014.01.012>.
- [13] Mat, Nor Azian Aini, Norihan Md Arifin, Roslinda Nazar, and Norfifah Bachok. "Boundary layer stagnation-point slip flow and heat transfer towards a shrinking/stretching cylinder over a permeable surface." *Applied Mathematics* 6, no. 3 (2015): 466-475. <https://doi.org/10.4236/am.2015.63044>.
- [14] Khashi'ie, Najiyah Safwa, Iskandar Waini, Nurul Amira Zainal, Khairum Hamzah, and Abdul Rahman Mohd Kasim. "Hybrid nanofluid flow past a shrinking cylinder with prescribed surface heat flux." *Symmetry* 12, no. 9 (2020): 1493. <https://doi.org/10.3390/sym12091493>.
- [15] Awaludin, Izyan Syazana, Rokiah Ahmad, and Anuar Ishak. "On the stability of the flow over a shrinking cylinder with prescribed surface heat flux." *Propulsion and Power Research* 9, no. 2 (2020): 181-187. <https://doi.org/10.1016/j.jprr.2020.03.001>.
- [16] Kardri, Mahani Ahmad, Norfifah Bachok, Norihan Md Arifin, Fadzilah Md Ali, and Yong Faezah Rahim. "Magnetohydrodynamic flow past a nonlinear stretching or shrinking cylinder in nanofluid with viscous dissipation and heat generation effect." *J. Adv. Res. Fluid Mech. Therm. Sci* 90 (2022): 102-114. <https://doi.org/10.37934/arfmts.90.1.102114>.
- [17] Choi, S. US, and Jeffrey A. Eastman. *Enhancing thermal conductivity of fluids with nanoparticles*. No. ANL/MSD/CP-84938; CONF-951135-29. Argonne National Lab.(ANL), Argonne, IL (United States), 1995. <https://www.osti.gov/biblio/196525>.
- [18] Arifin, Norihan Md, Roslinda Nazar, and Ioan Pop. "Viscous flow due to a permeable stretching/shrinking sheet in a nanofluid." *Sains Malaysiana* 40, no. 12 (2011): 1359-1367.
- [19] Wang, C. Y. "Stagnation flow towards a shrinking sheet." *International Journal of Non-Linear Mechanics* 43, no. 5 (2008): 377-382. <https://doi.org/10.1016/j.ijnonlinmec.2007.12.021>.
- [20] Tiwari, Raj Kamal, and Manab Kumar Das. "Heat transfer augmentation in a two-sided lid-driven differentially heated square cavity utilizing nanofluids." *International Journal of heat and Mass transfer* 50, no. 9-10 (2007): 2002-2018. <https://doi.org/10.1016/j.ijheatmasstransfer.2006.09.034>.
- [21] Bachok, Norfifah, Anuar Ishak, and Ioan Pop. "Boundary-layer flow of nanofluids over a moving surface in a flowing fluid." *International Journal of Thermal Sciences* 49, no. 9 (2010): 1663-1668. <https://doi.org/10.1016/j.ijthermalsci.2010.01.026>.
- [22] Makinde, Oluwale D., and Abdul Aziz. "Boundary layer flow of a nanofluid past a stretching sheet with a convective boundary condition." *International Journal of Thermal Sciences* 50, no. 7 (2011): 1326-1332. <https://doi.org/10.1016/j.ijthermalsci.2011.02.019>.
- [23] Bachok, Norfifah, Anuar Ishak, and Ioan Pop. 2012. "Unsteady Boundary-Layer Flow and Heat Transfer of a Nanofluid over a Permeable Stretching/Shrinking Sheet." *International Journal of Heat and Mass Transfer* 55 (7–8): 2102–9. <https://doi.org/10.1016/j.ijheatmasstransfer.2011.12.013>.
- [24] Bachok, Norfifah, Anuar Ishak, and Ioan Pop. "Unsteady boundary-layer flow and heat transfer of a nanofluid over a permeable stretching/shrinking sheet." *International Journal of Heat and Mass Transfer* 55, no. 7-8 (2012): 2102-2109. <https://doi.org/10.1186/1687-2770-2013-39>.
- [25] Iijima, Sumio. "Helical microtubules of graphitic carbon." *nature* 354, no. 6348 (1991): 56-58. <https://doi.org/10.1038/354056a0>.

- [26] Halelfadl, Salma, Thierry Maré, and Patrice Estellé. "Efficiency of carbon nanotubes water based nanofluids as coolants." *Experimental Thermal and Fluid Science* 53 (2014): 104-110. <https://doi.org/10.1016/j.expthermflusci.2013.11.010>.
- [27] Norzawary, Nur Hazirah Adilla, Norfifah Bachok, and Fadzilah Md Ali. "Stagnation point flow over a stretching/shrinking sheet in a carbon nanotubes with suction/injection effects." *CFD Letters* 12, no. 2 (2020): 106-114.
- [28] Mahabaleshwar, U. S., K. N. Sneha, A. Chan, and Dia Zeidan. "An effect of MHD fluid flow heat transfer using CNTs with thermal radiation and heat source/sink across a stretching/shrinking sheet." *International Communications in Heat and Mass Transfer* 135 (2022): 106080. <https://doi.org/10.1016/j.icheatmasstransfer.2022.106080>.
- [29] Samat, Nazrul Azlan Abdul, Norfifah Bachok, and Norihan Md Arifin. "The significant effect of hydromagnetic on carbon nanotubes based nanofluids flow and heat transfer past a porous stretching/shrinking sheet." *J. Adv. Res. Fluid Mech. Therm. Sci* 106, no. 1 (2023): 51-64. <https://doi.org/10.37934/arfmts.106.1.5164>.
- [30] Nasir, Saleem, Saeed Islam, Taza Gul, Zahir Shah, Muhammad Altaf Khan, Waris Khan, Aurang Zeb Khan, and Saima Khan. "Three-dimensional rotating flow of MHD single wall carbon nanotubes over a stretching sheet in presence of thermal radiation." *Applied Nanoscience* 8, no. 6 (2018): 1361-1378. <https://doi.org/10.1007/s13204-018-0766-0>.
- [31] Yacob, Nor Azizah, Nor Fadhilah Dzulkifli, Siti Nur Alwani Salleh, Anuar Ishak, and Ioan Pop. "Rotating flow in a nanofluid with CNT nanoparticles over a stretching/shrinking surface." *Mathematics* 10, no. 1 (2021): 7. <https://doi.org/10.3390/math10010007>.
- [32] Gari, Abdullatif A., Nazrul Islam, Sakeena Bibi, Aaqib Majeed, Kashif Ali, Wasim Jamshed, Kashif Irshad, Sohail Ahmad, and Sayed M. El Din. "A thermal case study of three dimensional MHD rotating flow comprising of multi-wall carbon nanotubes (MWCNTs) for sustainable energy systems." *Case Studies in Thermal Engineering* 50 (2023): 103504. <https://doi.org/10.1016/j.csite.2023.103504>.
- [33] Eswaramoorthi, S., Saleem Nasir, K. Loganathan, M. Satyanarayana Gupta, and Abdallah Berrouk. "Numerical simulation of rotating flow of CNT nanofluids with thermal radiation, ohmic heating, and autocatalytic chemical reactions." *Alexandria Engineering Journal* 113 (2025): 535-550. <https://doi.org/10.1016/j.aej.2024.10.124>.
- [34] Allaw, Dhurgham, Norfifah Bachok, Norihan Md Arifin, and Fadzilah Md Ali. "Double solutions of unsteady stagnation-point of Carbon Nanotubes across a permeable exponential stretching/shrinking sheet." *Chinese Journal of Physics* 85 (2023): 534-552. <https://doi.org/10.1016/j.cjph.2023.03.018>.
- [35] Mahapatra, T. Roy, and A. S. Gupta. "Magnetohydrodynamic stagnation-point flow towards a stretching sheet." *Acta Mechanica* 152, no. 1 (2001): 191-196. <https://doi.org/10.1007/BF01176953>.
- [36] Aman, Fazlina, Anuar Ishak, and Ioan Pop. "Magnetohydrodynamic stagnation-point flow towards a stretching/shrinking sheet with slip effects." *International communications in heat and mass transfer* 47 (2013): 68-72. <https://doi.org/10.1016/j.icheatmasstransfer.2013.06.005>.
- [37] Anuar, Nur Syazana, Norfifah Bachok, Norihan Md Arifin, and Haliza Rosali. "MHD flow past a nonlinear stretching/shrinking sheet in carbon nanotubes: Stability analysis." *Chinese journal of physics* 65 (2020): 436-446. <https://doi.org/10.1016/j.cjph.2020.03.003>.
- [38] shak, Anuar, Roslinda Nazar, and Ioan Pop. "Magnetohydrodynamic (MHD) flow of a micropolar fluid towards a stagnation point on a vertical surface." *Computers & Mathematics with Applications* 56, no. 12 (2008): 3188-3194. <https://doi.org/10.1016/j.camwa.2008.09.013>.
- [39] Uddin, Ziya, Korimerla Sai Vishwak, and Souad Harmand. "Numerical duality of MHD stagnation point flow and heat transfer of nanofluid past a shrinking/stretching sheet: Metaheuristic approach." *Chinese Journal of Physics* 73 (2021): 442-461. <https://doi.org/10.1016/j.cjph.2021.07.018>.
- [40] Yasin, Mohd Hafizi Mat, Anuar Ishak, and Ioan Pop. "MHD heat and mass transfer flow over a permeable stretching/shrinking sheet with radiation effect." *Journal of Magnetism and Magnetic Materials* 407 (2016): 235-240. <https://doi.org/10.1016/j.jmmm.2016.01.087>.
- [41] Patel, Harshad R., Akhil S. Mittal, and Rakesh R. Darji. "MHD flow of micropolar nanofluid over a stretching/shrinking sheet considering radiation." *International Communications in Heat and Mass Transfer* 108 (2019): 104322. <https://doi.org/10.1016/j.icheatmasstransfer.2019.104322>.
- [42] Yashkun, Ubaidullah, Khairy Zaimi, Nor Ashikin Abu Bakar, Anuar Ishak, and Ioan Pop. "MHD hybrid nanofluid flow over a permeable stretching/shrinking sheet with thermal radiation effect." *International Journal of Numerical Methods for Heat & Fluid Flow* 31, no. 3 (2021): 1014-1031. <https://doi.org/10.1108/HFF-02-2020-0083>.
- [43] Zhang, Xiao-Hong, Awatef Abidi, A. El-Sayed Ahmed, M. Riaz Khan, M. A. El-Shorbagy, Meshal Shutaywi, Alibek Issakhov, and Ahmed M. Galal. "MHD stagnation point flow of nanofluid over a curved stretching/shrinking surface subject to the influence of Joule heating and convective condition." *Case Studies in Thermal Engineering* 26 (2021): 101184. <https://doi.org/10.1016/j.csite.2021.101184>.

- [44] Vishalakshi, A. B., U. S. Mahabaleshwar, and Ioannis E. Sarris. "An MHD fluid flow over a porous stretching/shrinking sheet with slips and mass transpiration." *Micromachines* 13, no. 1 (2022): 116. <https://doi.org/10.3390/mi13010116>.
- [45] Khan, W. A., Z. H. Khan, and M. Rahi. "Fluid flow and heat transfer of carbon nanotubes along a flat plate with Navier slip boundary." *Applied Nanoscience* 4, no. 5 (2014): 633-641. <https://doi.org/10.1007/s13204-013-0242-9>.
- [46] Oztop, Hakan F., and Eiyad Abu-Nada. "Numerical study of natural convection in partially heated rectangular enclosures filled with nanofluids." *International journal of heat and fluid flow* 29, no. 5 (2008): 1326-1336. <https://doi.org/10.1016/j.ijheatfluidflow.2008.04.009>.